Lawrence Berkeley National Laboratory
Recent Work

Title
DESIGN AND PERFORMANCE CHARACTERISTICS OF A SENSITIVE CARBON MONOXIDE OPTOACOUSTIC DETECTOR

Permalink
https://escholarship.org/uc/item/2cz4v08k

Author
Gerlach, Robert

Publication Date
1977-08-01

LBL-6818
c.2

Energy and Environment Division

Design and Performance Characteristics
of a Sensitive Carbon Monoxide
Optoacoustic Detector

Robert Gerlach and Nabil M. Amer

August 1977

Lawrence Berkeley Laboratory   University of California/Berkeley

LBL-6818

DISCLAIMER

Design and Performance Characteristics of a Sensitive
Carbon Monoxide Optoacoustic Detector

Robert Gerlach and Nabil M. Amer

Applied Laser Spectroscopy Group
Lawrence Berkeley Laboratory
and
Physics Department
University of California
Berkeley, CA   94720

Abstract

Laser optoacoustic detection of carbon monoxide with a sensitivity of 0.15 parts per million has been achieved. A carbon monoxide laser oscillating on transitions in the fundamental 1→0 band, intensity modulated by means of an electro-optic modulator, was used. The performance of acoustically resonant and nonresonant optoacoustic cells was compared, and it was found that the minimum detectable concentration was lower for the resonant cell, but that the nonresonant cell was more suitable for operation at pressures below atmospheric pressure. The pressure dependence of the optoacoustic signal is discussed in the context of atmospheric absorption.

I. Introduction

In this report we describe an optoacoustic system for sensitive and interference free detection of carbon monoxide by optical resonance absorption. The system consisted of three basic subsystems: the coherent light source, the intensity modulator, and the optoacoustic cell. The light source was a cw carbon monoxide laser emitting several milliwatts on single transitions in the fundamental $1 \rightarrow 0$ band. Intensity modulation was achieved with an electro-optic modulator. Two types of optoacoustic cells were investigated: an acoustically nonresonant cell which was operated in its $1/f$ frequency response region, and a resonant cell which was driven at the frequency of its first radial resonance. Each of the subsystems will be described further in subsequent sections.

The resonant cell has a sensitivity of 0.15 ppm, limited by electronic noise. The sensitivity achieved with the nonresonant cell was approximately 1.5 parts per million (ppm), limited chiefly by a background signal attributed to window and/or wall heating by the beam. We have investigated the system's ability to discriminate against potential interferers and found it to be excellent.

II. The Laser

We used a cw gas discharge carbon monoxide laser[1] capable of oscillating on transitions in the 1→0 band of CO, around 4.75 μm. For sensitive and interference free detection of CO, operation on transitions in the 1→0 band was essential because only these wavelengths are resonantly, and hence strongly, absorbed by CO molecules in their ground vibrational state. Laser transitions in higher vibrational bands of CO are generally not resonant with transitions in the fundamental 1→0 band of CO, and while resonant with hot band transitions, these latter produce very little absorption at typical ambient temperatures.

Use of a grating end reflector on the CO laser enabled us to achieve lasing at a single wavelength, making possible excellent selectivity. Table 1 lists the laser lines used. Also observed, but not tabulated, were the $P_{1-0}(8)$ and $P_{1-0}(12)$ transitions, which lased too weakly to be useful. Two transitions in the 2→1 band have been included. The $P_{2-1}(8)$ transition is very far from the nearest 1→0 absorption line, and hence could give an indication of the level of background signal due to window and wall heating. The $P_{2-1}(12)$ transition has an accidental near coincidence with the $P_{1-0}(18)$ absorption line. The offset of the absorption line from the laser line is only 0.045 cm^{-1},[2] while the full width at half maximum absorption for CO lines in the 1→0 band pressure broadened by 1 atm of air is typically 0.10 to 0.14 cm^{-1}.[3] The absorption at this wavelength is weaker than for the resonant 1→0 transitions, but this is compensated for by the higher power available at this wavelength. However, it will be seen that there are other disadvantages to use of this non-resonant transition.

III. Modulation System

An electro-optic modulator was used to give vibration-free intensity modulation of the laser light. A standard system consisting of a quarter-wave plate, electro-optic crystal, and polarizer was used. The CdTe electro-optic crystal was of dimensions 6mm × 6mm × 50mm and had a half-wave voltage of about 2.85 kV at 4.753 μm. Both the modulate and the quarter-wave plate were antireflection coated for wavelengths around 4.75 μm, but in spite of this, the maximum transmission through the system was only about 67%, with most of the losses being traced to the quarter-wave plate. The polarizer consisted of multiple ZnSe plates at Brewster's angle. A 38 cm focal length lens was used to focus the laser beam into the modulator. Beyond the focal point of the lens, the beam divergence was 6 mrad half-angle at $1/e^2$ intensity, and the beam diameter where it reached the optoacoustic cell was 10 mm at $1/e^2$ intensity. A mirror behind the cell passed the beam back through to increase the amount of power absorbed in the cell. An overview of the optical configuration is shown in Fig. 1.

The modulator was driven with an approximately sinusoidal waveform obtained from an oscillator, audio frequency power amplifier, and 24 secondary : 1 primary turns ratio transformer. Since the modulator has a sinusoidal transfer characteristic, a sinusoidal input will result in an intensity modulation waveform consisting of a series of harmonics of the input frequency with Bessel function coefficients. The input voltage amplitude V_m which maximizes the first harmonic content of the modulation waveform is theoretically $V_m = 0.586 \, V_\pi = 1.67$ kV, where V_π is the half-wave voltage; the empirically determined optimum voltage was 1.75 kV.

IV. Optoacoustic Cells

Two types of optoacoustic cells were employed for comparison. The first was an acoustically nonresonant cell constructed from a copper pipe tee. It had a length of 7.6 cm and a diameter of 2.5 cm. The side branch of the tee, and a tube extending from it, housed the General Radio model 1961-9601 1-inch electret condenser microphone sensitivity 11 mV/Pa and 1972-9600 preamplifier. Sodium chloride windows were epoxied to the ends of the cell.

The cell was sandwiched between lead blocks, surrounded with acoustical shielding material, and enclosed in a plywood box resting on rubber foam for isolation from sound and vibrations. This resulted in only electrical noise being significant.

The noise spectrum observed for the system under normal operating conditions is plotted in Fig. 2. Also shown in the same figure is a portion of the frequency response curve of the cell, plotted in arbitrary units. At higher frequencies the cell was found to have longitudinal resonances at 2250 Hz, 4500 Hz, etc., but these longitudinal resonances are very weakly exicted at low concentration due to the uniformity with which power is deposited along the length of the cell. The first radial resonance of the cell was predicted to lie somewhat above 16 kHz, but we have been unable to observe it, possibly due to poor microphone response at that frequency.

We chose to operate at 25 Hz, a frequency at which both the opto-acoustic signal and the noise have an approximately 1/f frequency dependence. At this frequency the RMS noise was approximately 270 $nV/Hz^{1/2}$. When measuring small concentrations we used a 10 sec time constant on our

lock-in amplifier, resulting in a noise level of 35 nV RMS. Over a long period of observation the output fluctuated over a ±50 nV span, and we took this as the limitation on signal measurement set by noise.

For comparison, a Knowles model BT-1759 miniature electret microphone with built-in FET was used in place of the GR microphone and preamp. Comparison at the same frequency of 25 Hz was not meaningful because the Knowles microphone had a low-frequency cutoff around 50 Hz. At 100 Hz the Knowles microphone produced roughly the same signal as the GR microphone, as would be expected from the manufacturer's specifications, but its noise was larger by a factor of 6. Thus, compared under identical conditions, the Knowles microphone is inferior to the GR. Its advantage, however, is that, because of its small dimensions, it can be incorporated into a miniature optoacoustic cell, giving an enhancement in signal inversely proportional to the volume.

The other optoacoustic cell used in this experiment was an acousti-cally resonant cylindrical cavity of 10.8 cm in length and diameter, constructed of brass. The first radial resonance of this cell was observed at 3952 Hz, with a Q (defined as the resonant frequency divided by the full width at $1/\sqrt{2}$ response) of 760. A Knowles microphone was incorporated onto the cylindrical wall midway down the length of the cell. Because of its small size, the microphone did not degrade the Q of the cavity. Acoustical noise isolation precautions similar to those used with the nonresonant all were taken. The peak noise excursions at the resonant frequency with a 10 sec time constant were ±5.5 nV.

The system was calibrated by measuring the optoacoustic signals for gas mixtures of known CO concentration. We used certified gas mixtures

from National Bureau of Standards having concentrations 49.3±0.5,

95±0.9, and 476±5 parts per million, and mixtures from Matheson having

concentrations 6, 11, and 29 ppm of CO in N_2. (Uncertainties were ±5%

for the Matheson mixtures.) Mixtures of other concentrations were pre-

pared by diluting the NBS mixtures with N_2. Both gases were allowed to

flow into the cell simultaneously, and the mixing ratio was determined

from the flow rates of the individual gases. Care was taken to insure

proper and complete mixing.

V. Results

A typical measurement consisted of the following steps: First, the laser power at a point after the lens but before the quarter-wave plate was measured with a thermopile, while simultaneously a small part of the beam was split off and directed into a spectrometer with a PbSe detector at the exit slit, for identification of the laser line. The PbSe detector signal was recorded. Signal from the PbSe detector was used to monitor changes in the laser's output power. The optoacoustic signal was measured, divided by the power measured with the thermopile, and multiplied by a correction factor obtained from the change in the PbSe detector signal from the time of the power measurement to the time of the optoacoustic signal measurement. In spite of these efforts, the power normalization was still the primary source of error at high CO concentrations. Measurements were carried out for each of the laser transitions listed in Table 1.

Figure 3 shows plots of typical optoacoustic signal per milliwatt of laser output power as a function of CO concentration observed with the nonresonant cell for different laser wavelengths. The graphs exhibit a linear dependence on CO concentrations, with no clearcut indication of satuation at high concentration. At low concentration the signal levels off at a value several times the noise level of the system. This was an optoacoustic signal which disappears when the laser beam was blocked. It was also observed with pure N_2 in the cell. We attribute this background signal to heating of the windows and/of walls of the cell by the laser radiation.

Table 2 summarizes the data obtained with the nonresonant cell. Included are the following parameters for each laser line employed: the

signal per milliwatt per ppm of CO in the linear region, the CO concentration at which the linear curve intersects the constant background level, and the CO concentration at which the linear curve would intersect the noise level assuming the typical power levels listed in Table 1 for each line. An exception was made for the $P_{2-1}(12)$ line, where the maximum rather than the typical power was used because the typical power was for a non-optimized laser gas mixture.

In practice our limit of lowest detectable concentration was set by the background signal, which for the three resonant transitions allowed detection of about 1.5 ppm. For the $P_{2-1}(12)$ the absorption by CO was much weaker but the power available was much larger, so that at a given concentration, about the same signal to noise ratio could be achieved as for the resonant transitions. However, the higher power resulted in the effects of background due to window/wall heating becoming important at much higher concentration, around 15 ppm. Other disadvantages to the use of this nonresonant transition will be pointed out later.

The $P_{2-1}(8)$ transition is almost 1 cm^{-1} from the nearest CO absorption resonance, and at low concentrations, only the background is observed for this transition. Above about 100 ppm the signal does begin to increase linearly with CO concentration. The 2→1 hot band would not be expected to give significant absorption until much higher concentrations. However, the tail of the $P_{1-0}(14)$ absorption line is estimated to give about the right amount of absorption to account for the observed signal, in spite of the large offset in frequency.

In the case of the resonant cell, for a concentration of 49.3 ppm the signal for the $P_{1-0}(10)$ transitions was 0.37 μV/mW, so that the

signal per unit concentration was 7.5 nV/(mW ppm). With a 10 sec time
constant, giving a noise level of 5.5 nV, the concentration giving a
signal to noise ratio of unity is 0.15 ppm. No background signal was
seen above noise, so the minimum detectable concentration was limited
only by the noise. To determine the background signals, the laser was
tuned to a transition at 5.000 μm, where an output power of 225 mW could
be obtained. At that wavelength, the background was 1.4 nV/mW, so that
if the background at 4.75 μm were about the same, the equivalent concen-
tration producing the same signal would be about 0.19 ppm, comparable to
the noise-equivalent concentration.

We investigated the dependence of the optoacoustic signal on pres-
sure for both cells, since in the presence of interference, use of low
pressure might be desirable. For the acoustically nonresonant cell, as
the pressure of the $CO-N_2$ mixture was reduced from 760 torr to 75 torr,
the signal observed for the resonant $1\rightarrow0$ laser transitions was found to
be nearly independent of pressure, increasing slightly as pressure was
decreased. This is reasonable since in the pressure-broadened regime,
for constant percentage of absorbing gas, the absorption coefficient at
line center remains constant. Below 75 torr the signal fell off rapidly
as Doppler broadening began to dominate, causing the absorption coefficient
at line center to decrease in proportion to the pressure. For the opti-
cally nonresonant transition, $P_{2-1}(12)$, in the range from ~200 torr to
760 torr the signal was observed to fall off linearly with decreasing
pressure due to the narrowing of the absorption line. At lower pressures
the signal appeared to vary as a higher power of pressure. For an inter-
fering species whose absorption line did not coincide closely with the

laser line, the optoacoustic signal would have a pressure dependence

similar to that described for the $P_{2-1}(12)$ transition. By lowering the

pressure, the interfering absorption line is narrowed, and unless it is

in very close coincidence with the laser wavelength, its absorption will

be decreased. In contrast, the absorptivity of the resonantly absorbing

gas to be detected remains constant, independent of pressure, until

Doppler broadening begins to dominate. Hence, selectivity is improved

as pressured is decreased.

In the case of the acoustically resonant cell, even for an optically

resonant transition, the signal was found to depend linearly on pressure,

even though the absorbed power is independent of pressure in the pressure-

broadened regime. The reason is that as pressure decreased, the Q of the

acoustical resonance decreases. Although the sensitivity of this system

to an interfering species will then be decreased relative to the resonantly

absorbing gas by decreasing the pressure, the signal to noise ratio will

be degraded.

Thus, it appears that the acoustically nonresonant cell has an advan-

tage for lower pressure operation, since the signal, and hence signal to

noise ratio, remains constant as pressure is decreased, whereas for the

resonant cell, it falls off linearly with decreasing pressure. Also, the

background signal, which limits the sensitivity of the nonresonant cell at

atmospheric pressure, has been found to depend approximately linearly on

pressure, and would be less troublesome for low pressure operation.

To assess the effect of interference from atmospheric absorption,

we estimated atmospheric absorption coefficients for each of the laser

transitions from computer-generated atmospheric transmission spectra.[4]

For atmospheric pressure, temperature of 296°K, and relative humidity of 65%, these coefficients were compared to our estimated absorption coefficients to obtain equivalent CO concentrations which would result in the same absorption. The equivalent concentrations were 0.25 ppm for $P_{1-0}(9)$, 0.09 ppm for $P_{1-0}(10)$, 0.08 ppm for $P_{1-0}(11)$, and 0.43 ppm for $P_{2-1}(12)$. Due to the 0.25 cm^{-1} resolution folded into the computed spectra,[4] the equivalent CO concentrations may be somewhat higher for the $P_{1-0}(9)$ and $P_{1-0}(10)$ transitions, since these appear to lie close to the centers of atmospheric absorption lines, where finite resolution would result in an underestimate of the absorption coefficient. On the other hand, the $P_{1-0}(11)$ and $P_{2-1}(12)$ absorption coefficients are more likely to be overestimated since these lines lie far from the centers of atmospheric absorption lines.

While the atmospheric absorption coefficient for the $P_{2-1}(12)$ transition is not large, it appears as a high equivalent CO concentration due to the weak absorption of CO at that wavelength. Use of low pressures to eliminate this interference is not practicable because, as discussed above, it is not a resonantly absorbed transition.

Of the four transitions we have investigated, $P_{1-0}(11)$ offers the best combination of sensitivity and freedom from interference.

Recent combustion studies have shown that N_2O can be a serious interferer in determining the concentration of CO with monitoring instruments using broad-band, incoherent light sources (e.g., nondispersive infrared analyzers.)[5] The interference stems from the overlap of the 4.5 μm and 4.67 μm absorption bands of N_2O and CO, respectively. This finding motivated us to test the selectivity of our detector since, in

principle, detection by resonance absorption should result in the
unambiguous determination of CO concentration. We tested a mixture of
4200 ppm of N_2O in N_2 at atmospheric pressure using our acoustically non-
resonant detector and observed no signals above the usual background
level. We also tested a mixture of 4200 ppm of N_2O and 49 ppm of CO
and found that the observed optoacoustic signals did correspond to those
obtained for 49 ppm of CO in the complete absence of N_2O.

The sensitivity which we have been able to achieve has been limited
in part by the low power avaiable from our laser. If sensitivity is
noise limited, as in the case of the acoustically resonant cell, then an
improvement in sensitivity could be achieved by using a higher power laser.
In this context it is of interest to point out that a chemical laser
capable of emitting almost a Watt on transitions in the 1→0 band of CO has
been reported.[6] The use of such laser would easily extend our detectivity
to the sub-ppb levels. In addition, although the resonant cell presently
gives a higher signal to noise ratio, the amplitude of the pressure
fluctuation is higher in the nonresonant cell, and could be made still
higher by going to a lower frequency. With the present electronics this
would not result in any benefit because the electronic noise also goes
as $1/f$. However, if the signal could be translated in frequency to a
region where the amplifier noise was very low, while still retaining the
higher amplitude associated with the low modulation frequency, a great im-
provement in signal to noise ration could be achieved. This can be
achieved by incorporating a capacitance microphone into a balanced
a.c. bridge which is exicted with a high frequency. Pressure fluctua-
tions which change the microphone capacitance then drive the bridge out

of balance, and hence the high frequency signal measured across the bridge is modulated at the low frequency of the pressure fluctuation. This scheme provides an escape from 1/f noise, and is the method used in capacitance manometers.

Detection of CO with a sensitivity of better than about 1 ppm is not essential for pollution monitoring. However, improvements in technique such as suggested above may be essential for detection of atmospheric gases such as ammonia, which is present at the ppb level. We are currently developing such an approach, and others, for the ultra-sensitive optoacoustic detection of atmospheric NH_3.

Finally, we would like to point out that the tunability of the CO laser gives our system the versatility to detect other pollutants in addition to CO, most importantly nitric oxide (NO). Also, there are prospects for miniaturization of the system by use of a waveguide CO laser.

Acknowledgments

References

1. N. M. Amer and R. Garlach, "A Stable 1→0 CO Laser," LBL-598; (1977); N. Djeu, "CW single-line CO laser on the v = 1→v = 0 band," Appl. Phys. Lett. $\underline{23}$, 309 (1973).

2. T. R. Tood, C. M. Clayton, W. B. Telfair, T. K. McCubbin and J. Pliva, "Infrared Emission of $^{12}C^{16}O$, $^{13}C^{16}O$, and $^{12}C^{18}O$," J. Mol. Spectrosc. $\underline{62}$, 201 (1976).

3. R. T. Ku, E. D. Hinckley, and J. O. Sample, "Long-Path Monitoring of Atmospheric Carbon Monoxide with a Tunable Diode Laser System," Appl. Opt. $\underline{14}$, 854 (1976).

4. R. J. Nordsfrom, J. H. Shaw, W. R. Skinner, J. G. Calvert, W. H. Chan, and W. M. Uselman, "Computer-Generated Long-Path Air Spectra," EPA-600/3-77-026, available from Environmental Sciences Research Laboratory, E.P.A., Research Triangle Park, North Carolina 27711.

5. C. D. Hollowell and G. W. Traynor, to be published.

6. W. Q. Jeffers, H. Y. Ageno, C. E. Wiswall, and J. D. Kelley, "CW 1→0 Chemical Laser: Optical Pumping of CO," Appl. Phys. Lett. $\underline{29}$, 242 (1976).

Table 1. Characteristics of laser output in grating-tuned, single-line operation, and relation of laser lines to absorbing transitions of CO. Frequencies are from reference 2.

Laser line	Frequency (cm^{-1})	Maximum Power Observed (mW)	Typical Power (mW)	Nearest Absorbing Transition	Frequency (cm^{-1})
$P_{1-0}(9)$	2111.5434	3.7	2	$P_{1-0}(9)$	2111.5434
$P_{1-0}(10)$	2107.4231	6.5	5	$P_{1-0}(10)$	2107.4231
$P_{1-0}(11)$	2103.2688	8.1	5	$P_{1-0}(11)$	2103.2688
$P_{2-1}(8)$	2085.3418	10	7	$P_{1-0}(14)$	2086.3215
$P_{2-1}(12)$	2068.8025	51	18*	$P_{1-0}(18)$	2068.8476

*Maximizing power on $P_{2-1}(12)$ transition required adjustment of laser gas mixture, which was generally not done.

Table 2. Signal per unit power per unit concentration, background-equivalent concentration, and noise-equivalent concentration for the non-resonant cell.

Laser line	Signal per unit power per unit concentration (nV/(mW ppm))	Concentration below which background becomes dominant (ppm)	Extrapolated concentration for which signal =noise for typical laser power[*] (ppm)
$P_{1-0}(9)$	31.2	1.5	0.8
$P_{1-0}(10)$	27.7	1.5	0.4
$P_{1-0}(11)$	28.9	1.5	0.4
$P_{2-1}(8)$	0.09	100	80
$P_{2-1}(12)$	3.9	15	0.3[*]

[*]For the $P_{2-1}(12)$ transition the maximum power of 51 mW, rather than the typical power of 18 mW, was used, since a much higher "typical" power could have been obtained if the gas mixture had been optimized each time this transition was used.

Figure Captions

Fig. 1. Optical layout: T--laser tube; O--output mirror; B--beam

splitter; M--front surface mirror; L--lens; Q--quarter-wave

plate; E--electro-optic modulator; P--polarizer; C--optoacoustic

cell; I--acoustical isolation box.

Fig. 2. Noise spectrum and frequency response of the nonresonant

optoacoustic cell.

Fig. 3. Signal per unit power vs. concentration of CO in N_2 for the

nonresonant cell, for

a) $P_{1-0}(9)$

b) $P_{1-0}(10)$

c) $P_{1-0}(11)$

d) $P_{2-1}(8)$.

Fig. 4. Pressure dependence of the optoacoustic signal in the non-

resonant cell for a fixed relative concentration of CO in N_2,

for

a) a resonantly absorbed laser line, $P_{1-0}(10)$

b) a non-resonantly absorbed line, $P_{2-1}(12)$.
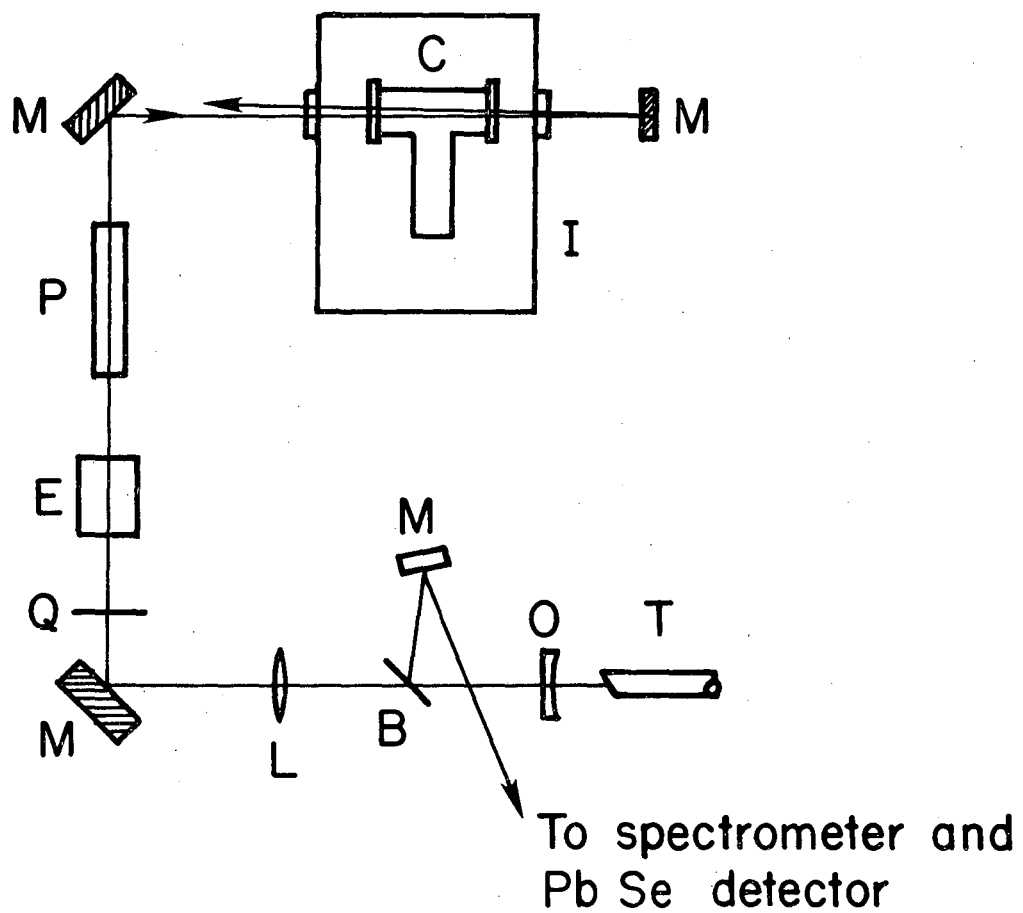
Fig. 1

XBL 779-1917
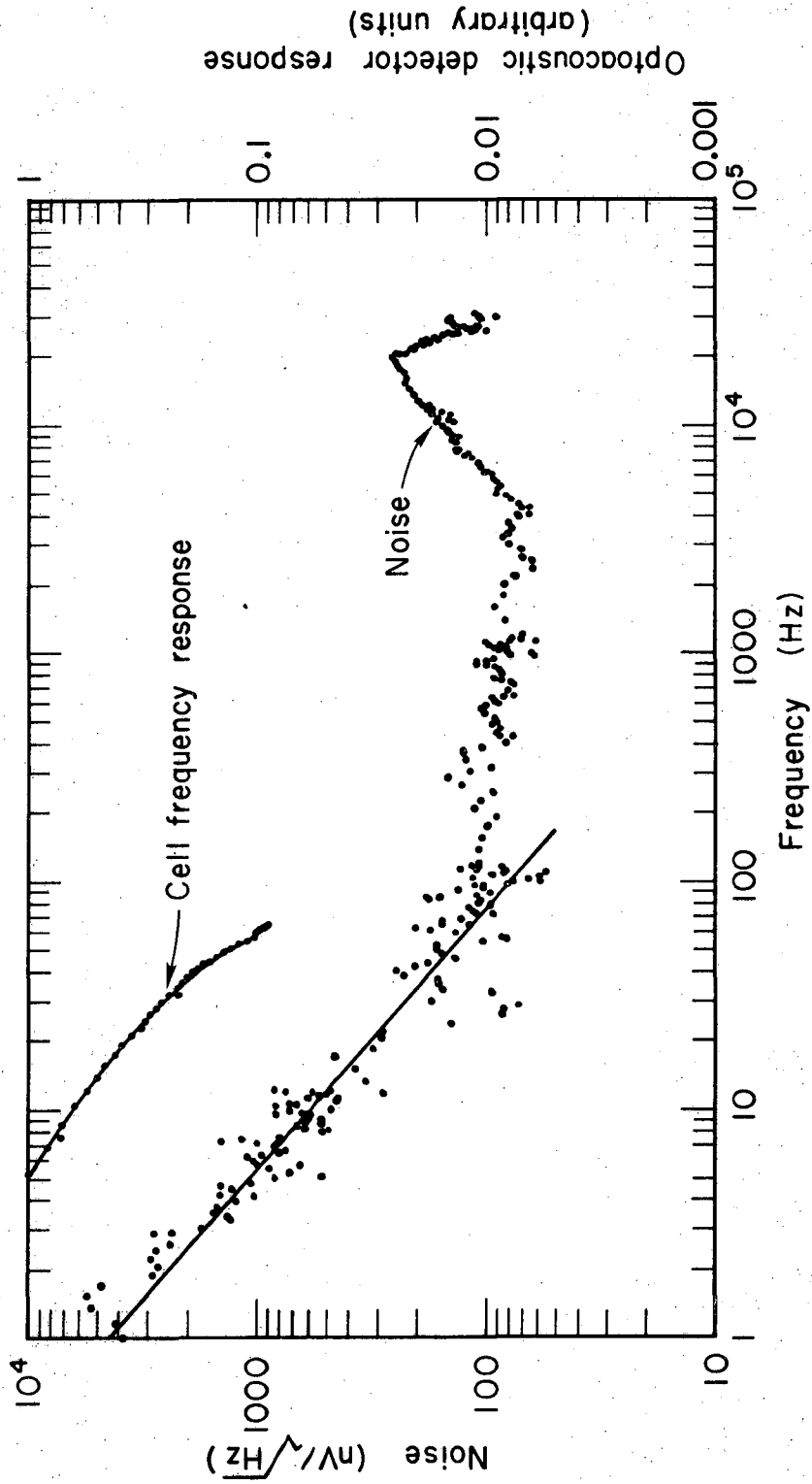
Fig. 2
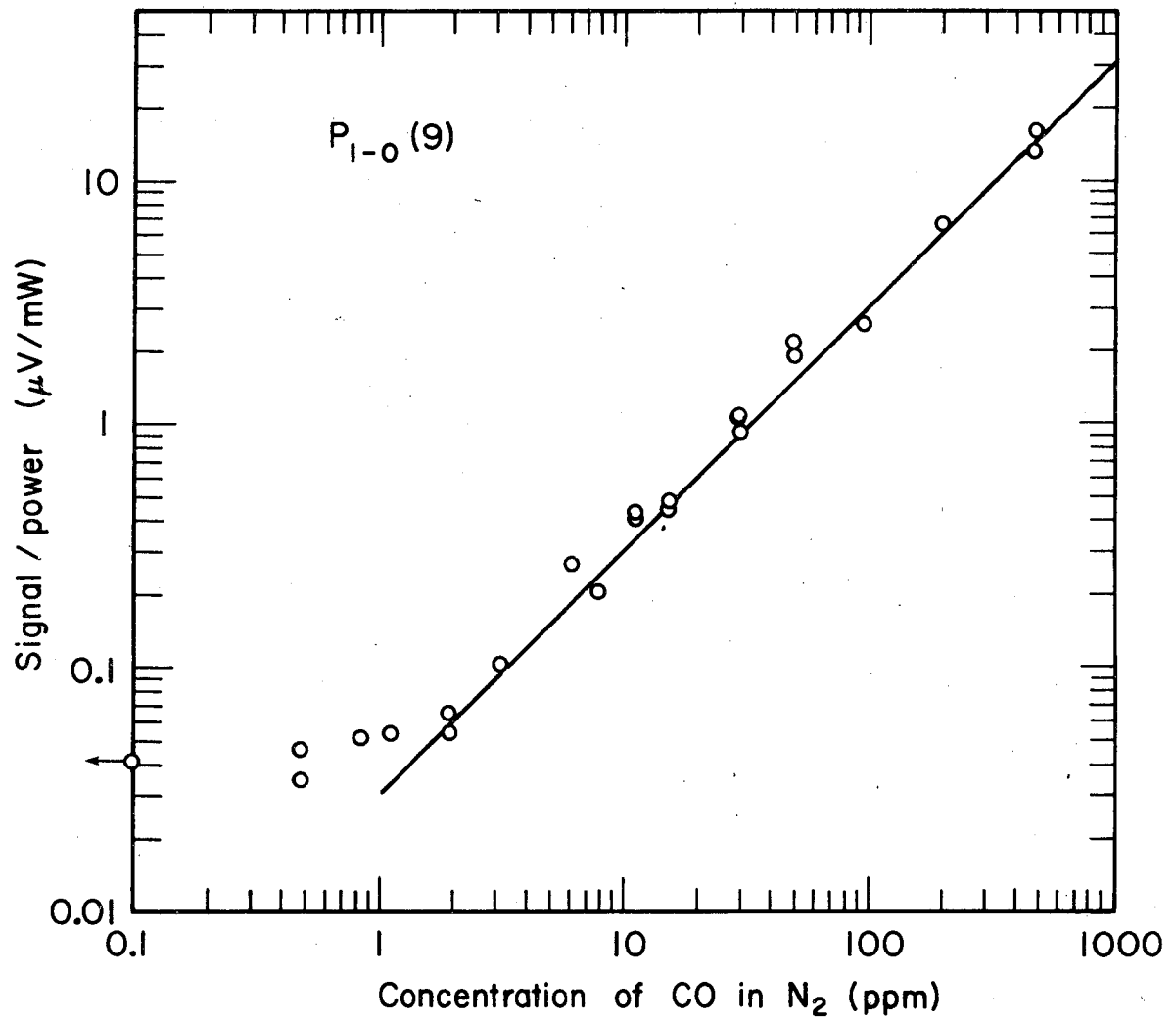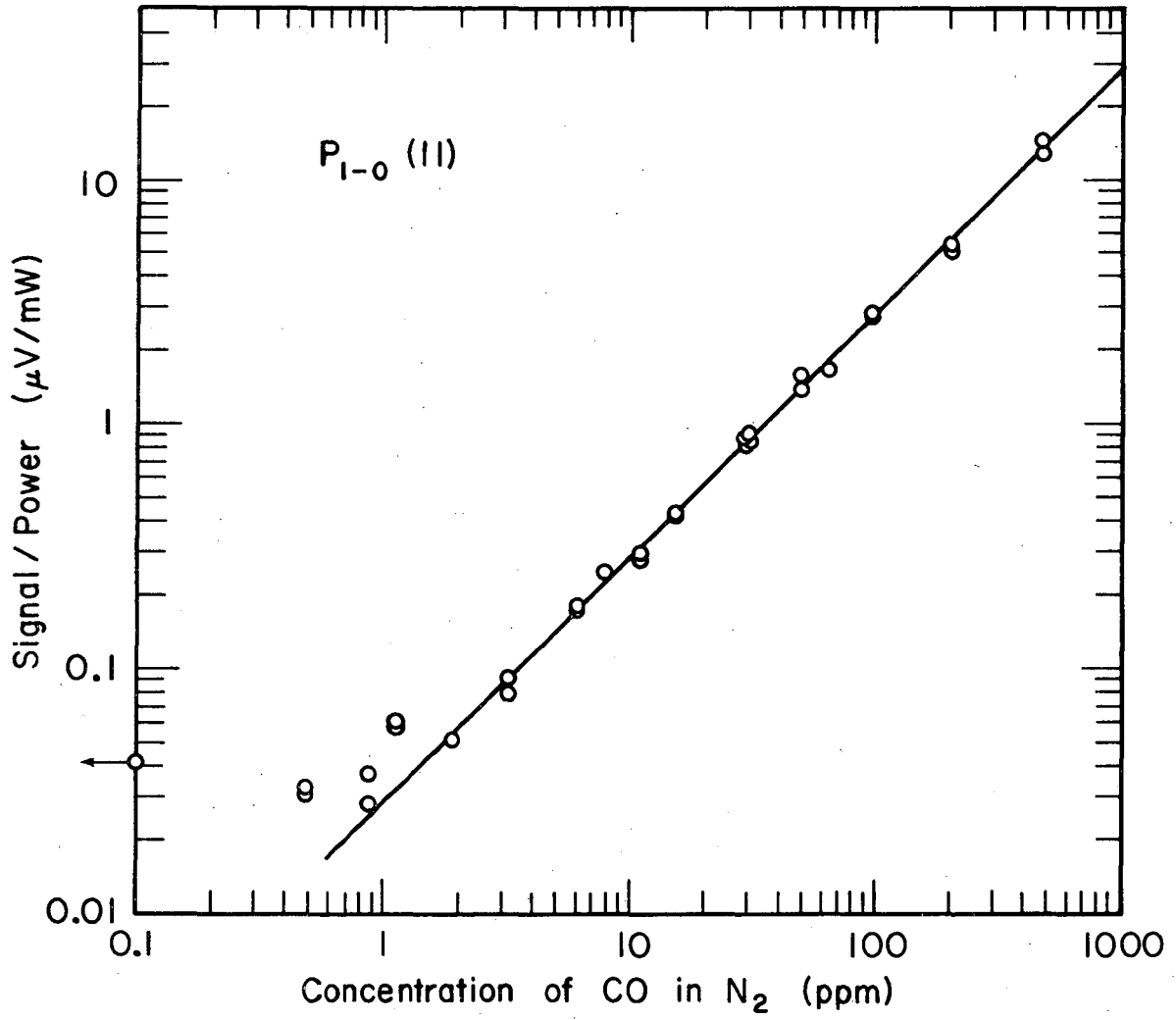
XBL 779-1916

Fig. 3a
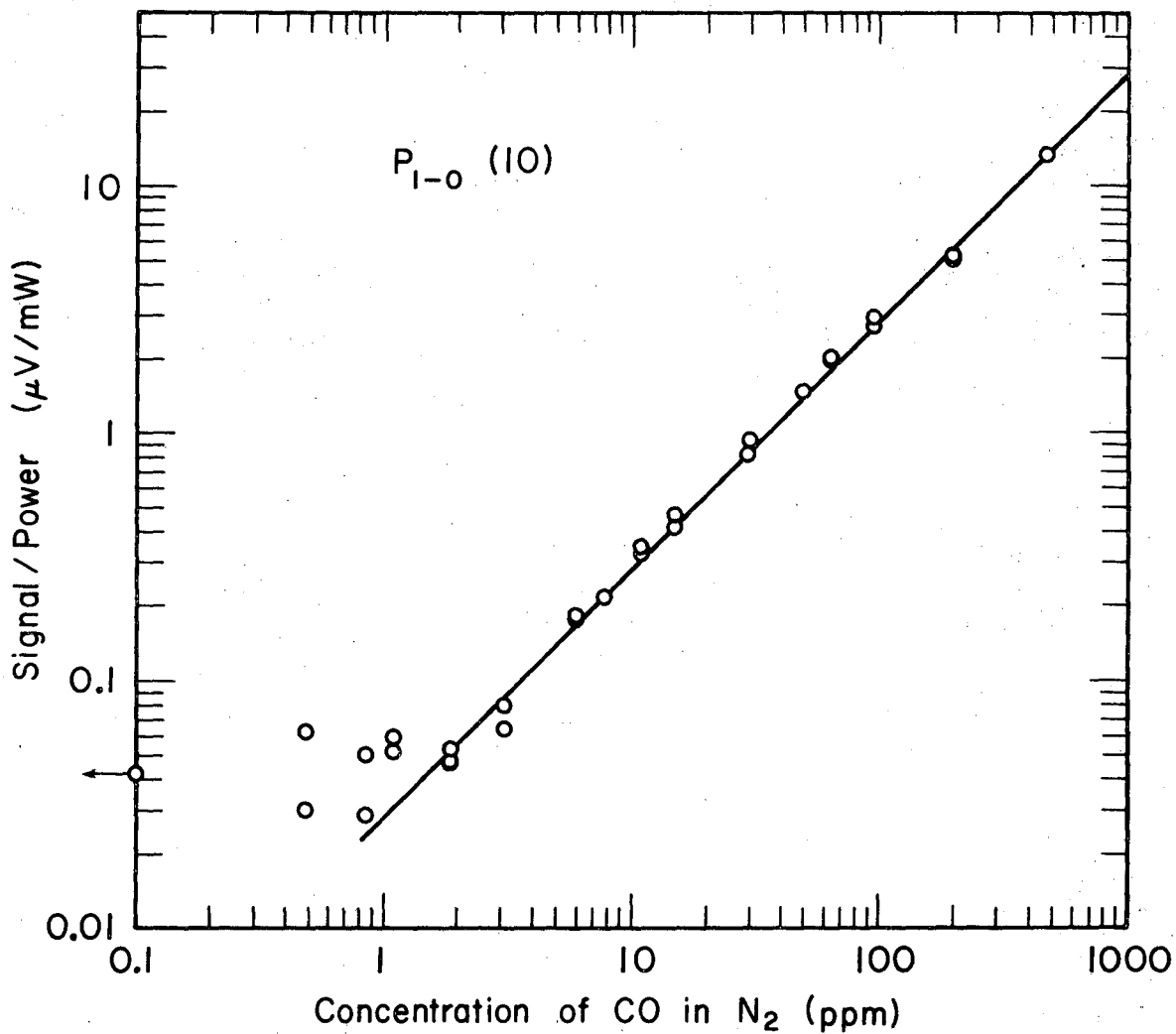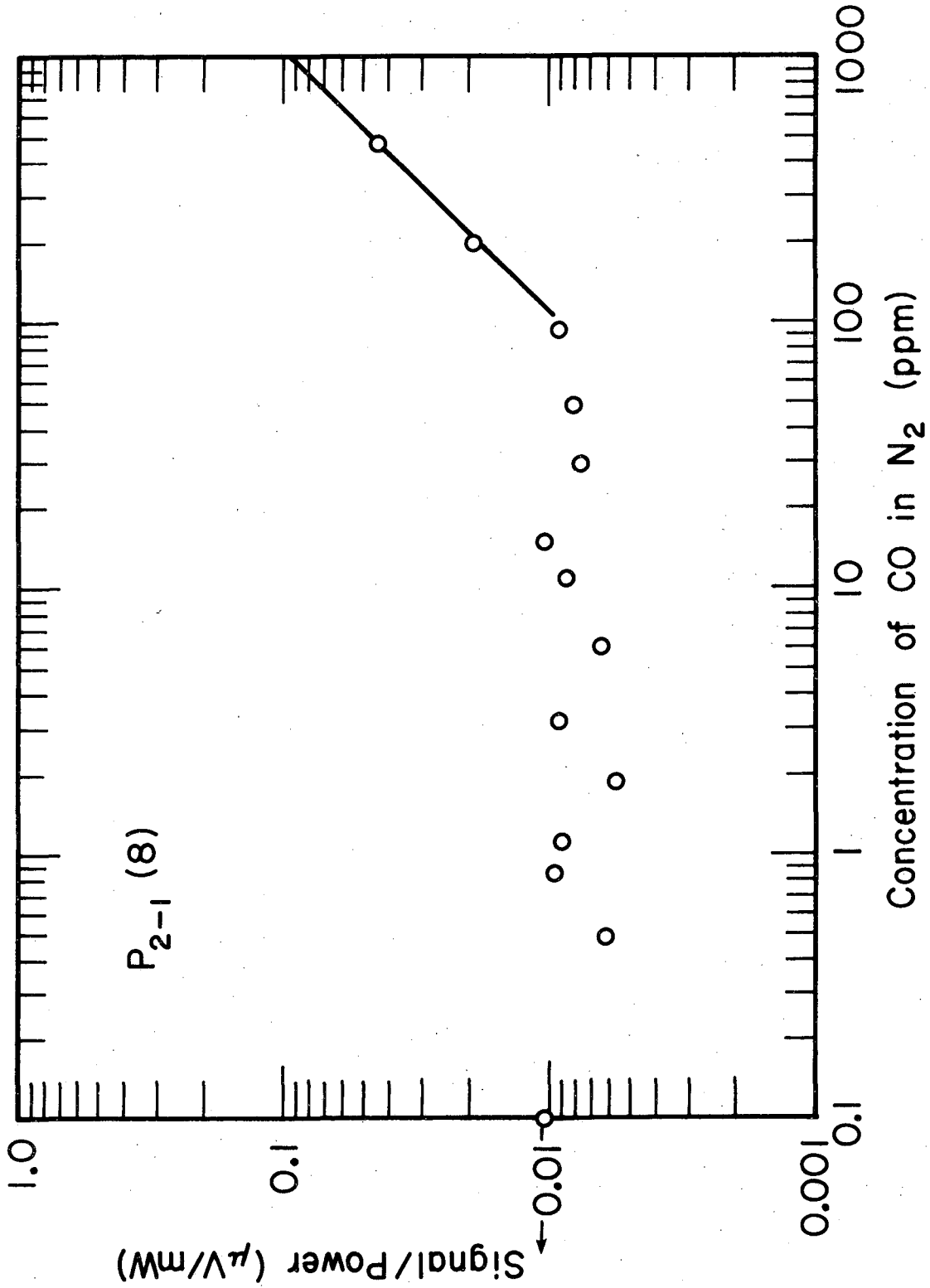
XBL 779-1918

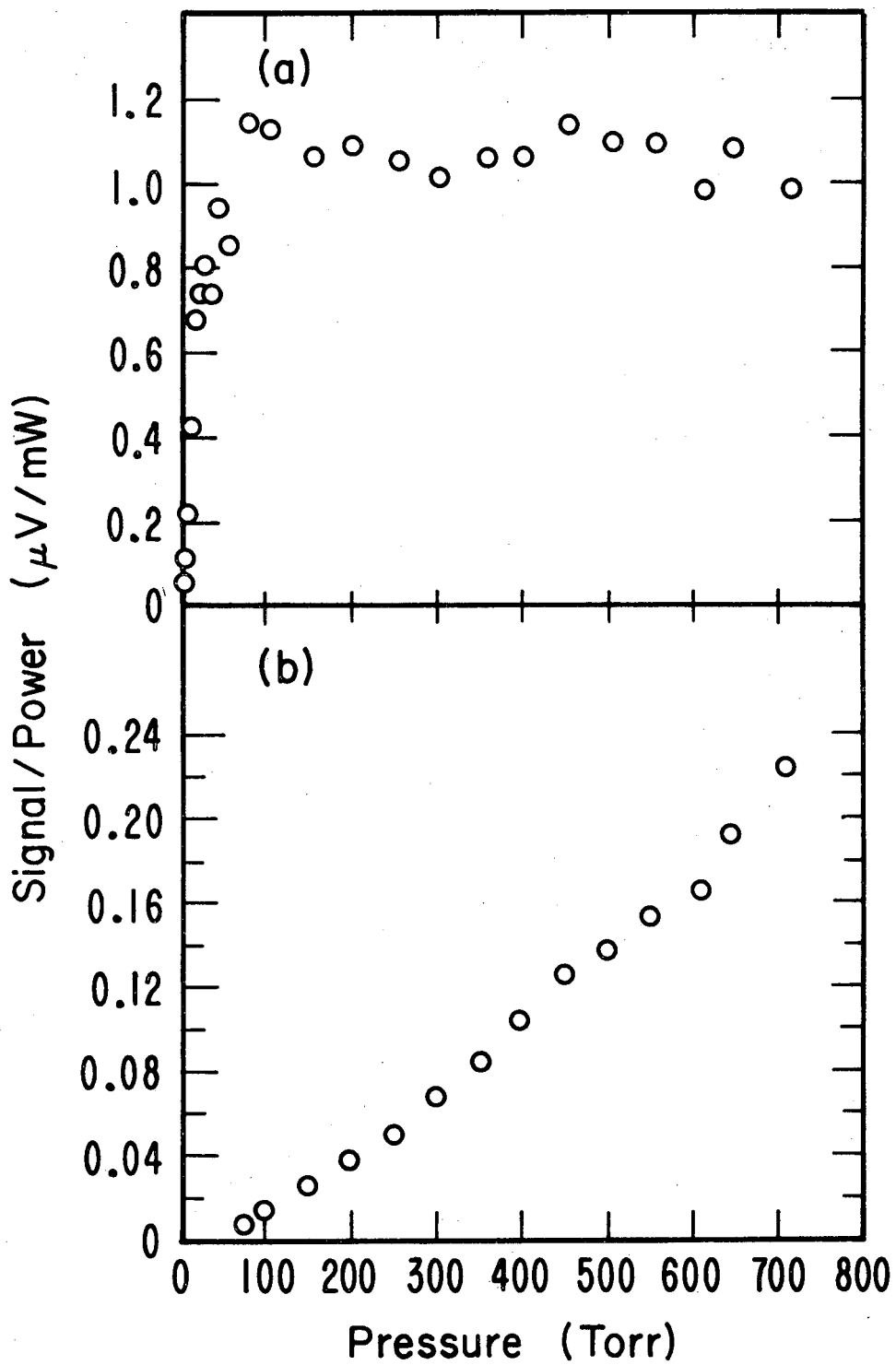Fig. 3b

XBL779-1919

Fig. 3c

XBL779-1920

Fig. 3d

XBL779-1921

Fig. 4

XBL 779-1923